Simulation of energetic particles driven Alfvén eigenmodes on EAST tokamak

BY YOUJUN HU

Institute of Plasma Physics, Chinese Academy of Sciences
Email: yjhu@ipp.cas.cn

1 Resonance condition of wave-particle interactions in toroidal geometries

For a general mode, the poloidal harmonics can be written as

$$A_m(\psi)e^{i(-\omega t+m\theta-n\phi)}, \tag{1}$$

where ω is the frequency of the mode, m and n are the poloidal and toroidal mode number, respectively. The phase variation seen by a particle when it goes one poloidal round is given by

$$-\omega T_\theta + m2\pi - n\Delta\varphi, \tag{2}$$

where T_θ is the period of the poloidal motion of the guiding center, $\Delta\varphi$ is the change of the toroidal angle during T_θ. For a particle to be resonant with the poloidal harmonics, the phase variation given by Eq. (2) should be multiple of 2π (is it necessary and/or sufficient?), i.e.,

$$-\omega T_\theta + m2\pi - n\Delta\varphi = 2\pi l, \tag{3}$$

with l being an integer. Dividing Eq. (3) by T_θ, we obtain

$$-\omega - n\omega_\varphi = (l-m)\omega_\theta \tag{4}$$

where $\omega_\theta = \frac{2\pi}{T_\theta}$ and $\omega_\varphi = \frac{\Delta\varphi}{T_\theta}$ are poloidal and toroidal angular frequency, respectively. The resonant condition given by Eq. (4) has been verified in Ref. [4].

1.1 Resonance condition between circulating particles and TAE

For a circulating particle, neglecting the guding orbit width and assuming the cange of $v_\parallel$ druing one poloidal period is small, the poloidal period is approximated by

$$T_\theta = \frac{2\pi Rq}{v_\parallel}. \tag{5}$$

Thus the poloidal frequency ω_θ is approximated by

$$\omega_\theta = \frac{2\pi}{T_\theta} = \frac{v_\parallel}{qR}. \tag{6}$$

The toroidal frequency is q times of the poloidal frequency, i.e.,

$$\omega_\varphi = q\omega_\theta = \frac{v_\parallel}{R}. \tag{7}$$

If the mode is a TAE, then the frequency and radial location are approximately given, respectively, by

$$\omega = \frac{V_A}{2q_{\rm gap}R}, \tag{8}$$

$$q_{\rm gap} = \frac{2m+1}{2n}. \tag{9}$$

Using Eqs. (6)-(9) in the resonance condition (4), we obtain

$$-\frac{nV_A}{(2m+1)R} - n\frac{v_\parallel}{R} = (l-m)\frac{2nv_\parallel}{(2m+1)R}, \tag{10}$$

which can be simplified to

$$-V_A = (2l+1)v_\parallel \tag{11}$$

For $l=0$

$$v_\parallel = V_A \tag{12}$$

For $l=1$

$$v_\parallel = -\frac{V_A}{3} \tag{13}$$

2 Energetic particles drive

$$\gamma \propto \frac{\partial f_0}{\partial E} + \frac{n}{\omega}\frac{\partial f_0}{\partial P_\varphi} \tag{14}$$

3 Research ideas: Determine which toroidal harmonics is the most unstable one on EAST tokamak

In MEGA code, the damping of AEs is modeled by the simple dispasitive coeeficients in the MHD equations. In this simple model, the dependence of the damping rate on the toroidal mode number n may not be correctly described. As a first approximation, we can assume that the damping rate is independent on the toroidal mode number n. Then the toroidal harmonics that have the maximum growth rate corresponds to the one which maximises the EPs drive.

When the radial extent of the eigenmodes is larger thant the orbit width, the EPs drive is proportional to the toroidal mode number n, as given by Eq. (14). With n increasing, the radial extent of the mode descreses. When the radial extent is small compared to the orbit width, the EPs drive will decrease with n increasing. Therefore there is an optimal toroidal mode number for which the EPs drive is maximised. This optimal toroidal number usually corresponds to $k_\theta\rho \sim 1$, where ρ is the orbit width of the resonace particles, k_θ is the poloidal wavenumber of the eigenmode.

(1) identify resonant particles, calculate its orbit width

(2) calculate the poloidal wavenumber of the most unstable mode.

(3) verify $k_\theta\rho \sim 1$ for the most unstable mode

4 Neutral beam injection on EAST tokamak

4.1 Injection geometry

In the EAST experiment campaign during 2014/06-2014/10, the neutral beam lies in the mid-plane and is injected in the co-current direction. The toroidal magnetic field is in the opposite direction of the current. The pitch angle of the fast ions generated by the NBI is defined by the included angle between the beam velocity and the magnetic field. Next, we estimate the pitch angle of the EAST NBI. Since the poloidal magnetic field is much smaller than the toroidal field, the pitch angle of the beam velocity with respect to the local magnetic field can be approximated as the included angle θ between the beam velocity and the toroidal direction. Using the definition of the tangential radius of the beams, the value of θ at at R can be calculated as

$$\theta(R) = \pi - \Big[\frac{\pi}{2} - \mathrm{Arcsin}(R_{\tan}/R)\Big]. \tag{15}$$

Using this formula, we obtain, at $R = 1.8$ (correspond approximately to the location of the magnetic axis), the pitch angle of the beam with $R_{\tan} = 1.26m$ is $\theta = 134.43°$; the pitch angle of the beam with $R_{\tan} = 0.73$ is $\theta = 114.93°$. The averaged pitch angle of the two beams is approximated as $(134.43° + 114.93°)/2 = 124.68°$.

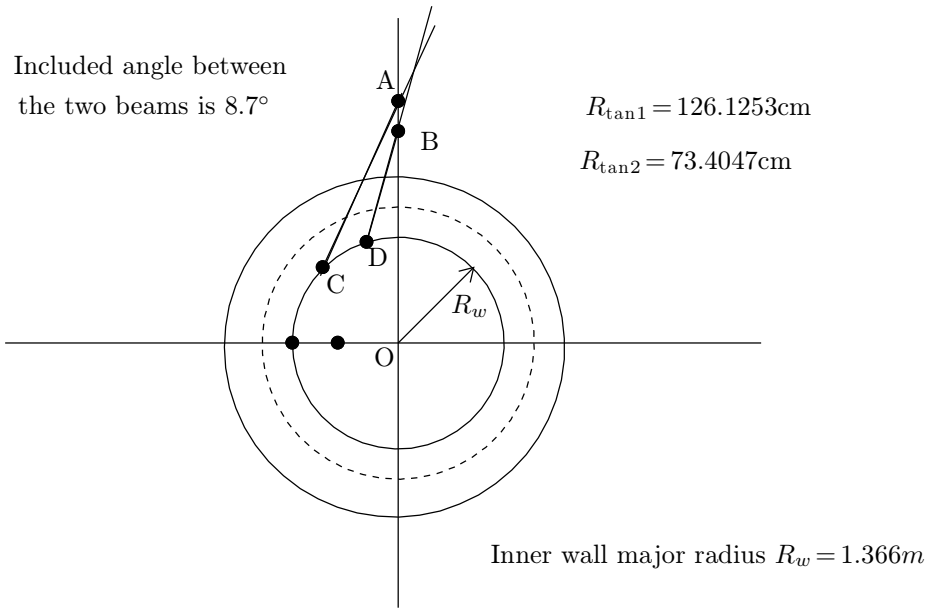

Figure 1. Top view of the neutral beam injection geometry on EAST tokamak. The two beams both lie in the midplane of the device, with the included angle between them being 8.7°. The tangential radius (the perpendicular distance from the axsymmetrical axis of the device to the beam line) of the two beams are 73.4047cm and 126.1253cm, respectively. Because the major radius of the inner wall of EAST ($R_w = 1.366m$) is larger than the tangential radius of the two beams, both the beam lines insect the inner wall. The current is in the count clockwise direction (top view) and the magnetic field is the clockwise direction (top view).

4.2 NBI fast ions distribution

The fast ions disdribution generated by NBI should be calculated by considering the process of ionizing and collisional transport of the generated fast ions. These processes can be modeled by the NUBEAM code. However, in this study, for the purpose to be simple, the distribution function of the fast ions is directly specified.

The isotropic "slowing down" distribution of fast ions is given by

$$f(v) = \begin{cases} \dfrac{1}{v^3 + v_{\text{crit}}^3} & \text{for } 0 < v \leqslant v_{\text{birth}} \\ 0 & \text{for } v > v_{\text{birth}} \end{cases}, \tag{16}$$

where v_{birth} is the birth velocity of the fast ions (for the 80keV Deuterium NBI on EAST $E_h =$ 80keV , $v_{\text{birth}} = \sqrt{2E_b/m_D} = 2.76 \times 10^6 m/s$), v_{crit} is the critical velocity for the collisional friction of fast ions with electrons and ions being equal, which is given by

$$v_{\text{crit}} = \left(\frac{m_e}{m_i} \frac{3\sqrt{\pi}}{4} \right)^{1/3} v_{te}, \tag{17}$$

(The derivation of Eq. (17) is given in Sec. 5.3.) For $T_e = 2\text{keV}$, $v_{\text{crit}} = 2.38 \times 10^6 m/s$. [In the numerical implementation, the jump of the distrbution function at $v = v_b$ is usually mimicked by the error function erfc, i.e., equation (16) is approximated by

$$f(v) = \frac{1}{v^3 + v_{\text{crit}}^3} \frac{1}{2} \text{erfc}\left(\frac{v - v_{\text{birth}}}{\Delta v} \right), \tag{18}$$

where erfc is the error function and Δv is set to a small value (in my simulation Δv chosen so that $\Delta v / V_A = 0.05$, where V_A is the Alfven speed at the magnetic axis).]

Define the normalized magnetic moment

$$\lambda = \frac{\mu B_0}{\varepsilon}, \tag{19}$$

where B_0 is the strength of the equilibrium magnetic field at the magnetic axis. Using the definition of the magnetic moment, equation (19) can be further written

$$\lambda = \frac{\frac{m v_\perp^2}{2B} B_0}{\varepsilon} = \frac{B_0}{B} \frac{m v_\perp^2}{m v^2} = B_0 \frac{\sin^2 \theta}{B}. \tag{20}$$

In terms of the midplane coordinates (v_0, θ_0), the above equation is written

$$\lambda = B_0 \frac{\sin^2 \theta_0}{B_{\min}}, \tag{21}$$

where $B_{\min}$ the strength of the magnetic field at the low-field-side of the midplane. Using $B_0 \approx B_{\min}$ and $\theta_0 \approx 124^\circ$ for EAST, we obtain $\lambda \approx 0.68$. [In the numerical implementation, the dependence of f on λ is assumed of the form

$$\exp\left(- \frac{(\lambda - \lambda_0)^2}{\Delta \lambda} \right), \tag{22}$$

where λ_0 and $\Delta\lambda$ are the centeal value of λ and the width of Gaussian function, respectively. In the simulation, I choose $\lambda = 0.68$ and $\Delta\lambda = 0.1$.]

The radial profile of the density of the fast ions is assumed of the form

$$\exp\left(- \frac{\psi^2}{\psi_{\text{scale}}} \right), \tag{23}$$

where ψ is the normalized poloidal flux and ψ_{scale} is the radial scale length. In the simulation, I choose $\psi_{\text{scale}} = 0.4$.

$$f(\psi, v, \lambda) = n(\psi) \frac{1}{v^3 + v_{\text{crit}}^3} \frac{1}{2} \text{erfc}\left(\frac{v - v_{\text{birth}}}{\Delta v} \right) \exp\left(- \frac{(\lambda - \lambda_0)^2}{\Delta \lambda} \right), \tag{24}$$

$$n(\psi) = n_0 \exp\left(- \frac{\psi}{\psi_{\text{scale}}} \right), \tag{25}$$

where the number density at the magnetic axis n_0 is chosen in the code to ahieve a desired beta value at the magnetic axis (this value can be set by users).

Use the EAST discharge #38300 at 3.9s as a reference equilibrium. The magnetic field strength at magentic axis is 1.63Tesla. The Alfvén velocity at the magnetic axis is $V_A = 3.835 \times 10^6 m/s$. For the 80keV Deuterium NBI on EAST, $v_{\text{birth}} = \sqrt{2E_b/m_D} = 2.76 \times 10^6 m/s$. The ratio of the beam velocity to the Alfvén velocity is

$$\frac{v_{\text{birth}}}{V_A} = \frac{2.76 \times 10^6}{3.835 \times 10^6} = 0.72 \tag{26}$$

EAST NBI: $4\text{MW} \times 10s$ @ 80keV

4.3 Normaliztion used in MEGA simulation

The time unit used in Mega simulation is $1/\Omega_h$, where $\Omega_h = B_0|q_h|/m_h$ is the cyclotron angular frequency of the energetic particles (EPs), B_0 is the strength of the magnetic field at the magnetic axis, q_h and m_h are the charge and the mass of the EPs. The velocity unit in Mega is the Alfvén speed at the magnetic axis, $V_{A0} = B_0/\sqrt{\mu_0\rho_{m0}}$, where ρ_{m0} is the mass density at the magnetic axis. Since both time unit and velocity unit has been chosen, the length unit used in Mega is a derived unit, which is defined by V_{A0}/Ω_f.

The magnetic field unit used in Mega is the strength of the magnetic field at the magnetic axis.

The Alfven time is defined by $t_A = R_0/V_{A0}$, where R_0 is the major radius of magnetic axis.

MEGA code (MHD+EPs hybrid codes)

$$f(\theta,t) = \sum_{m=0}^{\infty} A_m(t)\cos(m\theta) + \sum_{m=0}^{\infty} B_m(t)\sin(m\theta)$$

$$A_m\cos(m\theta) + B_m\sin(m\theta)$$

$$m = 1$$

$$m = 2$$

$$m = 3$$

4.4 Magnetic flux coordinates used in analyzing the MEGA simulation results

Flux coordinates (ψ, θ, ϕ) used in analyzing MEGA simulation results

Here ψ is the normalized poloidal flux
ϕ is the usual toroidal angle
θ is chosen to make magnetic field lines straight on (θ, ϕ) plane

proportional to ϕ along the magnetic field line so that the magnetic field lines are straight lines (with slope q) on (θ, ϕ) plane.

5 MEGA Simulation

5.1 Simulation parameters

Simulation performed in the cylindrical coordinates (R, ϕ, Z). Number of grids in (R, ϕ, Z) is $128 \times 128 \times 64$.

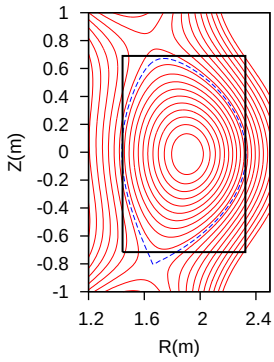

Figure 2. Flux surfaces shape and the compuational region of Mega simulation for EAST discharge #38300 at 3.9s. The center of the compuational region is chosen to be at ($R = R_0, Z = Z_{\rm axis}$), where R_0 is major radius of LCFS, $Z_{\rm axis}$ is the Z coordinate of the magnetic axis.

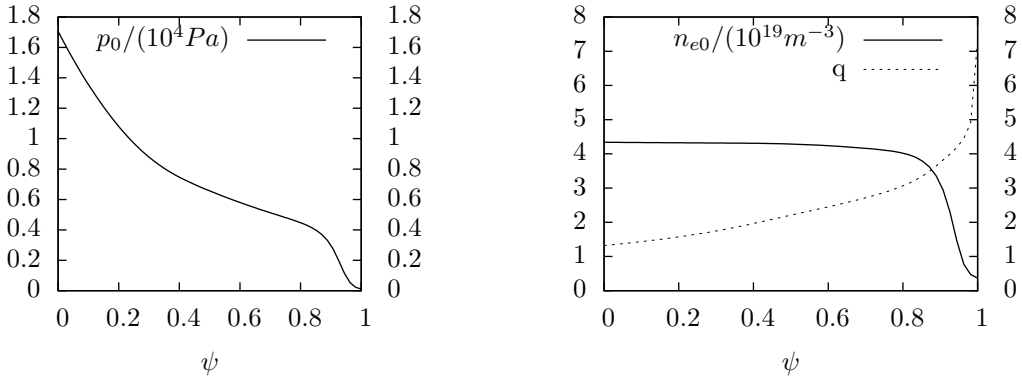

Figure 3. Profiles of the pressure (a), electron number density and safety factor (b) for EAST discharge #38300 at 3.9s.

5.2 Simulation results

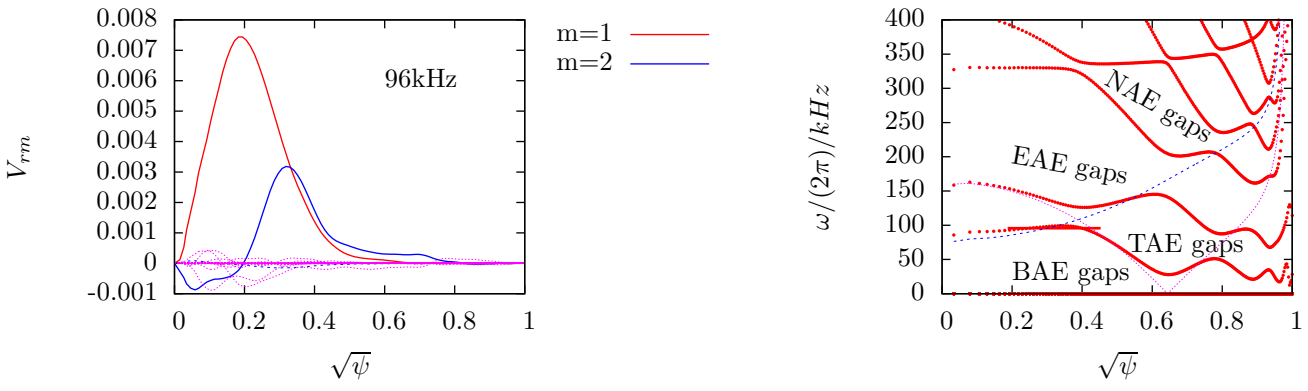

Figure 4. (a) $n = 1$ TAE mode structure and (b) $n = 1$ Alfven continua.

$$\frac{V_A}{R_0}$$

$$t = \bar{t}\,/\Omega_h = \bar{\tau}\,39.1/\Omega_h$$

$$0.0476243 \times 7.85009 \times 10^7/39.1 = 95.6151 \times 10^3$$

5.3 Derivation of the critical velocity

The velocity of the fast ions generated in NBI is much larger than the thermal velocity of ions but smaller than the electron thermal velocity, i.e,

$$v_{ti} \ll v_f < v_{te}. \tag{27}$$

For the α particles created in D-T reaction, the relation in Eq. (27) also applies. [The ratio of α particle's velocity to v_{te} is given by

$$\frac{v_\alpha}{v_{te}} = \sqrt{\frac{T_\alpha}{T_e}\frac{m_e}{m_\alpha}}. \tag{28}$$

For an electron temperature $T_e = 20\text{keV}$, the above equation gives

$$\frac{v_\alpha}{v_{te}} = \sqrt{\frac{3.5 \times 10^6\text{eV}}{20 \times 10^3\text{eV}}\frac{1}{1836}} = 0.304, \tag{29}$$

which indicates that the velocity of α particles are still smaller than the electron thermal velocity.] Next, we derive the criticle velocity of fast ions for which the collision friction of the fast ions with electrons and ions is equal. The collision friction coefficient due to an isotropic field-particles is given by[2]

$$F^{a/b}(v) = -\frac{4\pi\Gamma^{a/b}}{3n_b}\frac{m_a}{m_b}\frac{1}{v^2}\int_0^v 3(v')^2 f_b(v')dv', \tag{30}$$

where $\Gamma^{a/b} = \frac{n_b q_a^2 q_b^2}{4\pi\epsilon_0^2 m_a^2}\ln\Lambda^{a/b}$. Consider the collision friction of fast ions with thermal ions. Assume the distribution of thermal ions are Maxwellian, then Eq. (30) is written

$$F^{f/i}(v) = -\frac{4\pi\Gamma^{f/i}}{3n_i}\frac{m_f}{m_i}\frac{1}{v^2}\int_0^v 3(v')^2 f_{Mi}(v')dv'. \tag{31}$$

Since v_f is much larger than the thermal velcity of ions, the collision friction coefficients can be approximated by the high-velcity-limit (i.e. to set the upper limit of the integration to be $+\infty$), which gives

$$F^{f/i} = -4\pi\Gamma^{a/i}\frac{m_a}{m_i}\frac{1}{v^2}\left(\frac{m_i}{2\pi T_i}\right)^{3/2} v_{ti}^3\frac{\sqrt{\pi}}{4} \tag{32}$$

For the collision friction of fast ions with thermal electrons, since $v_f < v_{te}$, Eq. (30) is written

$$\begin{aligned} F^{f/e} &= -\frac{4\pi\Gamma^{a/e}}{n_e}\frac{m_a}{m_e}\frac{1}{v^2}\int_0^v (v')^2 f_{Me}(v')dv' \\ &= -\frac{4\pi\Gamma^{a/e}}{n_e}\frac{m_a}{m_e}\frac{1}{v^2}\int_0^v (v')^2 n_e\left(\frac{m_e}{2\pi T_e}\right)^{3/2}\exp\left(-\frac{v^2}{v_t^2}\right)dv' \\ &= -4\pi\Gamma^{a/e}\left(\frac{m_e}{2\pi T_e}\right)^{3/2}\frac{m_a}{m_e}\frac{v_t^3}{v^2}\int_0^x x^2\exp(-x^2)dx, \end{aligned} \tag{33}$$

where $x = v/v_{te}$. Sinc $x < 1$, we expand $e^{-x^2} \approx 1$. Using this, Eq. (33) is written

$$\begin{aligned} F^{f/e} &= -4\pi\Gamma^{a/e}\left(\frac{m_e}{2\pi T_e}\right)^{3/2}\frac{m_a}{m_e}\frac{v_{te}^3}{v^2}\int_0^x (x^2)dx \\ &= -4\pi\Gamma^{a/e}\left(\frac{m_e}{2\pi T_e}\right)^{3/2}\frac{m_a}{m_e}\frac{v_{te}^3}{v^2}\left(\frac{x^3}{3}\right) \end{aligned} \tag{34}$$

The critical velocity $v_{\rm crit}$ is given by the balance of $F^{f/i}$ and $F^{f/e}$, i.e. $F^{f/i} = F^{f/e}$. Using this, along with Eqs. (32) and (34), we obtain

$$-4\pi\Gamma^{a/i}\frac{m_a}{m_i}\frac{1}{v_{\rm crit}^2}\left(\frac{m_i}{2\pi T_i}\right)^{3/2}v_{ti}^3\frac{\sqrt{\pi}}{4} = -4\pi\Gamma^{a/e}\left(\frac{m_e}{2\pi T_e}\right)^{3/2}\frac{m_a}{m_e}\frac{v_{te}^3}{v_{\rm crit}^2}\left(\frac{v_{\rm crit}^3}{3v_{te}^3}\right),$$

Using $\Gamma^{a/b} = \frac{n_b q_a^2 q_b^2}{4\pi\epsilon_0^2 m_a^2}\ln\Lambda^{a/b}$ and $\ln\Lambda^{f/i} \approx \ln\Lambda^{f/e}$, the above equation is written

$$v_{\rm crit} = \left(\frac{n_i Z^2}{n_e}\frac{m_e}{m_i}\frac{3\sqrt{\pi}}{4}\right)^{1/3} v_{te},$$

which corresponds to the fast ions kinetic energy

$$E_{\rm crit} \equiv \frac{1}{2}m_f v_{\rm crit}^2 = \frac{m_f}{m_i}\left(\frac{m_i}{m_e}\right)^{1/3}\left(\frac{n_i Z^2}{n_e}\frac{3\sqrt{\pi}}{4}\right)^{2/3} T_e, \tag{35}$$

which agrees with the critical energy given in Ref. [1].

6 Coupling of EPs and MHD

The MHD momentum equation is given by

$$\rho\left(\frac{\partial \boldsymbol{u}}{\partial t} + \boldsymbol{u}\cdot\nabla\boldsymbol{u}\right) = Q_{\rm MHD}\boldsymbol{E} - \nabla p + \boldsymbol{J}_{\rm MHD}\times\boldsymbol{B}, \tag{36}$$

where $Q_{\rm MHD}$ and $\boldsymbol{J}_{\rm MHD}$ are the charge density and current density of the MHD plasma, respectively. For a system consisting of MHD plasma and energetic partilces, $Q_{\rm MHD}$ and $\boldsymbol{J}_{\rm MHD}$ are written as

$$Q_{\rm MHD} = Q - Q_h, \tag{37}$$

$$\boldsymbol{J}_{\rm MHD} = \boldsymbol{J} - \boldsymbol{J}_h, \tag{38}$$

where Q and Q_h are the total charge density and the charge density of EPs, respectively, $\boldsymbol{J}$ and $\boldsymbol{J}_h$ are the total current density and the current density of EPs, respectively. Using Eqs. (37) and (38), equation (36) is written

$$\rho\left(\frac{\partial \boldsymbol{u}}{\partial t} + \boldsymbol{u}\cdot\nabla\boldsymbol{u}\right) = (Q - Q_h)\boldsymbol{E} - \nabla p + (\boldsymbol{J} - \boldsymbol{J}_h)\times\boldsymbol{B}. \tag{39}$$

Thus, the charge density and current density of EPs are coupled to the MHD momentum equation.

Note that the MHD+EPs plasma system in tokamak device is created by three means, i.e., electromagnetic wave heating, neutral beam injection, and the fusion reactions. None of the three means introduce net charges into the plasma. Thus the total charge neutrality can be assumed. Further, we assume the local charge neutrality is valid, i.e., the total charge density of the MHD+EPs system is assumed to be zero, i.e., $Q = 0$. Using these, and noting that the total current density is given by $\boldsymbol{J} = (\nabla\times\boldsymbol{B})/\mu_0$, the momentum equation is written

$$\rho\left(\frac{\partial \boldsymbol{u}}{\partial t} + \boldsymbol{u}\cdot\nabla\boldsymbol{u}\right) = -Q_h\boldsymbol{E} - \nabla p + [(\nabla\times\boldsymbol{B})/\mu_0 - \boldsymbol{J}_h]\times\boldsymbol{B}. \tag{40}$$

The current density of energetic particles is given by

$$\boldsymbol{J}_h = \int (\boldsymbol{v}_\parallel^\star + \boldsymbol{v}_B + \boldsymbol{v}_E) Z_h e f d^3v - \nabla \times \int \mu \boldsymbol{b} f d^3v, \tag{41}$$

where $Z_h e$ the charge of the energetic particles, the last term is the magnetization current (which seems to be independent of the charge of the EPs, why?). Consider the current density contributed by the $\boldsymbol{E} \times \boldsymbol{B}$ drift, i.e., $\int \boldsymbol{v}_E f d^3v$, which can be written as

$$\int \left(\frac{1}{B_\parallel^\star} \boldsymbol{E} \times \boldsymbol{b} \right) Z_h e f d^3v. \tag{42}$$

Then the Lorentz force of this current is written

$$-\boldsymbol{B} \times \int \left(\frac{1}{B_\parallel^\star} \boldsymbol{E} \times \boldsymbol{b} \right) Z_h e f d^3v, \tag{43}$$

which can be further written as

$$\int \left[\frac{1}{B_\parallel^\star} (\boldsymbol{B} \cdot \boldsymbol{E}) \boldsymbol{b} - \frac{1}{B_\parallel^\star} B \boldsymbol{E} \right] Z_h e f d^3v, \tag{44}$$

Using that $B_\parallel^\star \approx B$ and $\boldsymbol{E}$ is approximately perpendicular to $\boldsymbol{B}$ (for ideal MHD, this is exact), the above expression is written as

$$-\boldsymbol{E} \int Z_h e f d^3v, \tag{45}$$

i.e., $-Q_h \boldsymbol{E}$. Using this in Eq. (40), we find that the electric force $Q_h \boldsymbol{E}$ happens to be canceled out, which yields

$$\rho \left(\frac{\partial \boldsymbol{u}}{\partial t} + \boldsymbol{u} \cdot \nabla \boldsymbol{u} \right) = -\nabla p + \left[(\nabla \times \boldsymbol{B})/\mu_0 - \boldsymbol{J}_h' \right] \times \boldsymbol{B}, \tag{46}$$

where

$$\boldsymbol{J}_h' = \int (\boldsymbol{v}_\parallel^\star + \boldsymbol{v}_B) Z_h e f d^3v - \nabla \times \int \mu \boldsymbol{b} f d^3v, \tag{47}$$

is the current density of EPs with the contribution of $\boldsymbol{E} \times \boldsymbol{B}$ drifts removed. Equations (46) and (47) are the MHD+EPs coupling model used in Mega simulation[3].

7 misc

7.1 Choose a computational coordinate system

7.1.1 Advantages and disadvantes of using magnetic surface coordinates in numerical simulation of tokamak plasmas

The magnetic surface coordinates are usually adopted for the numerical simulation of tokamak plasmas. Next, we discuss the advantages and disadvantages of using the magnetic surface coordinates in simulations. A class of wave modes in tokamak plasmas localized near some special magnetic surfaces (e.g. the resonant surfaces). In this case, if we use the magnetic surface coordinates, then we can restrict the compuational region to be near where the modes localize, thus reducing the compuational overhead. This is the most important advantage of using magnetic surface coordinates in simulations. Other advantages of using the magnetic surface coordinates includes that the results of computation can be conveniently interpreted from the physical prospective and the results can be conveniently compared with analytical theory since analytical theory usually uses magnetic coordinates. The disavantage of using magnetic surface coordinates includes that there is singularity at the origin of the coordinate system and thus a small region near the origin needs to be removed from the computational region and a computional boundary is needed on the resulting inner boundary.

7.1.2 Advantages and disadvantes of using cylindrical coordinates in numerical simulation of tokamak plasmas

The practical advantages of using the cylindrical coordinates in a numerical code include that (1) there is no singularity at the origin (2) the cylindrical coordinates are simple and it is easy to expresse most equations we encounter in these coordinates. The disadvantages of using the cylindrical coordinates include that (1) we will need more grids to resolve the wave modes that localize neare a magnetic surface; (2) the computational boundary on the poloidal plane is usually a rectangle and thus the flexibility of using different boundary shapes and seting different boundary conditions on the boundary is limited.

7.2 Instantaneous frequency and growth rate

Suppose $f(t)$ is a time dependent quantity given by

$$f(t) = A(t)\sin[\alpha(t)], \tag{48}$$

then the instantaneous angular frequency is given by

$$\omega = \frac{d\alpha}{dt}. \tag{49}$$

and the instantaneous growth rate is given by

$$\gamma = \frac{dA}{dt}. \tag{50}$$

Next consider a general poloidal harmonics

$$p(t) = a_m\cos(m\theta) + b_m\sin(m\theta), \tag{51}$$

where $a_m = a_m(t)$ and $b_m = b_m(t)$. Next we examine whether $p(t)$ can be written in the following form:

$$p(t) = A\sin(m\theta + \alpha), \tag{52}$$

By using the triangluar formula, equation (52) is written

$$p(t) = A\sin(\alpha)\cos(m\theta) + A\cos(\alpha)\sin(m\theta), \tag{53}$$

Comparing Eq. (53) with Eq. (51), we obtain

$$\sin(\alpha) = \frac{a_m}{A} \tag{54}$$

$$\cos(\alpha) = \frac{b_m}{A}. \tag{55}$$

The combinition of Eq. (54) and (55) implies that

$$1 = \left(\frac{a_m}{A}\right)^2 + \left(\frac{b_m}{A}\right)^2, \tag{56}$$

i.e.,

$$A^2 = a_m^2 + b_m^2, \tag{57}$$

i.e. (we choose the positive branch),

$$A = \sqrt{a_m^2 + b_m^2} \tag{58}$$

In summary, the general poloidal harmonics Eq. (51) can be written in the form (52) with the amplitude A given by Eq. (58) and the phase angle given by Eqs. (54) and (55). Therefore the instantaneous frequency and growth rate can be calculated by using Eqs. (49) and (50).

7.3 tmp

For 3.5MeV α particles created in D-T reaction, $v_{\text{birth}} = 1.295 \times 10^7 m/s$;
Write $p(t)$ in the form

$$\begin{aligned} p(t) &= a_m \cos(m\theta) + b_m \sin(m\theta) \\ &= A_m \cos(m\theta + \alpha), \qquad (59) \\ &= A_m \cos(\alpha)\cos(m\theta) - A_m \sin(\alpha)\sin(m\theta), \qquad (60) \end{aligned}$$

then it implies that

$$\cos(\alpha) = \frac{a_m}{A_m} \qquad (61)$$

$$\sin(\alpha) = -\frac{b_m}{A_m}. \qquad (62)$$

which further implies that

$$1 = \left(\frac{a_m}{A_m}\right)^2 + \left(\frac{b_m}{A_m}\right)^2,$$

i.e.,

$$A_m^2 = a_m^2 + b_m^2. \qquad (63)$$

$$\int_0^{v_{\text{birth}}} v^2 f(v) dv = \int_0^{v_{\text{birth}}} \frac{v^2}{v^3 + v_{\text{crit}}^3} dv = \frac{1}{3} \ln\left(1 + \frac{v_{\text{birth}}^3}{v_{\text{crit}}^3}\right) \qquad (64)$$

Bibliography

[1] Chapter 5: Physics of energetic ions. *Nucl. Fusion*, 39(12):2471, 1999.

[2] Charles F. F. Karney. Fokker-planck and quasilinear codes. *Comp. Phys. Rep.*, 4:183–244, 1986.

[3] Y. Todo. Properties of energetic-particle continuum modes destabilized by energetic ions with beam-like velocity distributions. *Physics of Plasmas (1994-present)*, 13(8):–, 2006.

[4] Y. Todo and T. Sato. Linear and nonlinear particle-magnetohydrodynamic simulations of the toroidal alfven eigenmode. *Phys. Plasmas*, 5(5), 1998.